Nuclear Engineering and Technology 51 (2019) 1828–1834

Contents lists available at ScienceDirect

Nuclear Engineering and Technology

journal homepage: www.elsevier.com/locate/net

Original Article

Fundamental approach to development of plastic scintillator system for in situ groundwater beta monitoring

UkJae Lee, Woo Nyun Choi, Jun Woo Bae, Hee Reyoung Kim*

Nuclear Engineering, Ulsan National Institute of Science and Technology, 50, UNIST-gil, Ulsan, 44919, Republic of Korea

ARTICLE INFO

Article history:
Received 18 December 2018
Received in revised form
16 April 2019
Accepted 3 May 2019
Available online 3 May 2019

Keywords:
Plastic scintillator
In situ measurement system
MCNP code simulation
Beta-emitting radionuclides

ABSTRACT

The performance of a plastic scintillator for use in an in situ measurement system was analyzed using simulation and experimental methods. The experimental results of four major pure beta-emitting radionuclides, namely ^{3}H, ^{14}C, ^{32}P, and $^{90}Sr/^{90}Y$, were compared with those obtained using a Monte Carlo *N*-particle (MCNP) code simulation. The MCNP simulation and experimental results demonstrated good agreement for ^{32}P and $^{90}Sr/^{90}Y$, with a relative difference of 1.95% and 0.43% between experimental and simulation efficiencies for ^{32}P and $^{90}Sr/^{90}Y$, respectively. However, owing to the short range of beta particles in water, the efficiency for ^{14}C was extremely low, and ^{3}H could not be detected. To directly measure the low-energy beta radionuclides considering their short range, a system where the source could flow directly to the scintillator was developed. The optimal thickness of the plastic scintillator was determined based on the suggested diameter. Results showed that the detection efficiency decreases with an increase in the depth of the water. The detection efficiency decreased drastically to approximately 10 cm, and the tendency was gradually constant.

1. Introduction

Radiological characterization during environmental restoration after the decommissioning of nuclear facilities is necessary to classify the waste generated from these activities and to determine whether the waste should be released freely or self-disposed using clearance materials, so that considerable radioactivity can be eliminated before the overall decommissioning of the site. In general, characterization of radioactive contamination at decommissioning sites has been performed using contamination sampling methods that involve laboratory measurements. However, such an analysis is time-consuming and results in a long delay between sample collection and result acquisition [1].

In Korea, research has been carried out in technical fields pertaining to in situ gamma spectroscopy and alpha-beta phoswich detectors to overcome the limitations of laboratory-based methods. However, gross beta measurement has not been considered in the context of water until recently. Therefore, we attempted to develop an in situ beta measurement system for decontamination and decommissioning (D&D) sites. A plastic scintillator exhibits little damage during contact with water and demonstrates high sensitivity when it is in direct contact with a radiation source to detect short-range beta radiation; based on these principles, a system for simultaneous monitoring of beta radiation including tritium in the groundwater of decommissioning sites has been proposed [2].

The plastic scintillator can affect the overall efficiency of a monitoring system because it converts radiation energy to photons. If the plastic scintillator does not convert radiation energy to photons well, the photo multiplier tubes (PMT) cannot accurately amplify the light, resulting in a decrease in the detection efficiency [3]. Therefore, before constructing a monitoring system, it is necessary to analyze the efficiency of the plastic scintillator. In this study, we calculated the efficiency of a plastic scintillator made of polystyrene by using a Monte Carlo *N*-particle (MCNP6) code simulation and compared the simulation results with experimental results obtained for four pure major beta-emitting radionuclides, ^{3}H, ^{14}C, ^{32}P, and ^{90}Sr, in aqueous form [4].

2. Experiment and simulation method

2.1. Experimental setup

To analyze the characteristics of underwater β-radionuclides in a D&D site and design a conceptual detection system (Fig. 1), a

* Corresponding author.
E-mail address: kimhr@unist.ac.kr (H.R. Kim).

https://doi.org/10.1016/j.net.2019.05.006

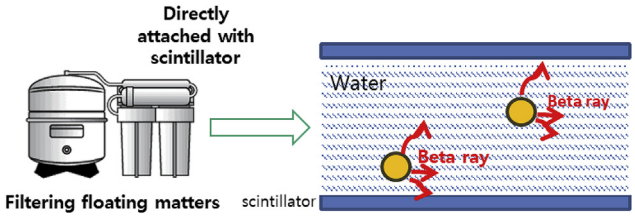

Fig. 1. Concept of in situ beta monitoring with plastic scintillator.

plastic scintillator and PMT R878 were used. A monitoring system was designed to detect beta radionuclides in water directly by applying a simple pretreatment process including the filtration of matter suspended in the water.

The PMT R878 device is illustrated in Fig. 2 (a) and Table 1 lists the device characteristics including its spectral response range and peak wave length [5]. Fig. 2 (b) shows the employed plastic scintillator, and Table 2 lists its characteristics such as the base material and wavelength of emission [6]. The plastic scintillator, which is physically and chemically stable, exhibits little damage during direct exposure to water and has relatively low back scattering owing to its low effective atomic number. The material used to build the scintillator was polystyrene because it has a better detection efficiency than other materials. In addition, the sensitivity of the scintillator to gamma rays is approximately 40% that of the sensitivity of NaI(TI); therefore, the background radiation level can be reduced.

Analyses of the spectral characteristics of ^{90}Sr and ^{14}C and analyses of tritium measurement characteristics using a disk-type plastic scintillator have previously been reported [7,8]. To directly measure low-energy beta nuclides such as ^{3}H, ^{14}C, and ^{32}P on-site, we designed a system that allows the source to flow directly to the scintillation material considering the short range of these particles. Fig. 3 shows range–energy curves for beta particles in various substances including water; the particles have a shorter range in water than in air. Eqs. (1) and (2) show the expressions to calculate the range according to the beta energy [9]. For example, because the beta energy of ^{90}Y, which is a daughter radionuclide of ^{90}Sr, is 2.284 MeV, Eq. (2) must be used; thus, the resulting range of ^{90}Y is 1.10 g/cm^2. The corresponding range in water can be obtained by dividing this result by the density of water (1 g/cm^3); the range in water in this case is 1.1 cm.

$$R = 0.407E^{1.38} \qquad E \leq 0.8MeV \tag{1}$$

$$R = 0.542E - 0.133 \qquad E \geq 0.8MeV \tag{2}$$

where R is the range in g/cm^2 and E is the maximum beta energy in MeV.

An NIM (Nuclear Instrumentation Module) based spectroscopy system was applied for the analysis and detection of beta nuclides (Fig. 4). This system is capable of ensuring that the source flows directly into the scintillator. The system was constructed using a 276 Photomultiplier Base with a Preamplifier, an 855 Dual Amplifier, a 551 Timing Single Channel Analyzer, a 567 Time-to-Amplitude Converter/SCA, and a 556 High Voltage Power Supply (AMETEK ORTEC, USA). Fig. 5 shows the process flow diagram of the detection signal processing system. The 556 HV Power Supply applies power to the 276 PM Base/Preamplifier; then, the 855 Amplifier performs photon amplification. These photons are then changed to a signal form when they pass through the 551 Timing SCA and 567 Time to Amplitude Converter. Subsequently, the total counts of radionuclides can be checked [10–14].

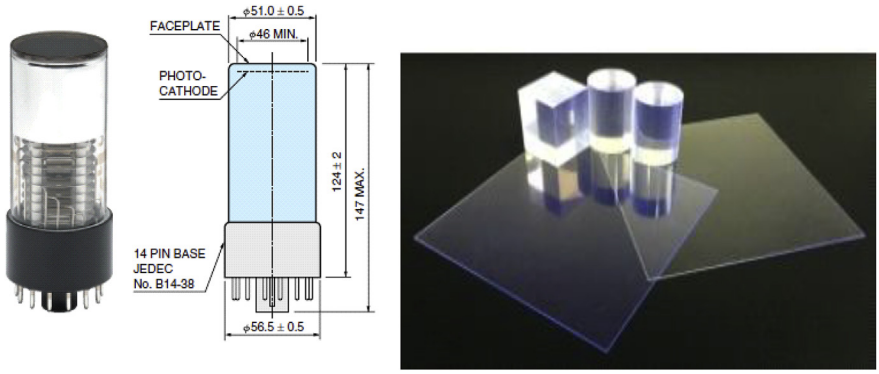

Fig. 2. PMT R878 (a) and plastic scintillator (b).

Table 1
Specifications of PMT-R878 (HAMAMATSU).

Spectral Response Range (nm)	Curve Code	Peak Wave-length (nm)	Photo-cathode Material	Window Material	Dynode Structure/Stages	Anode to Cathode Voltage (V)	Average Anode Current	Anode to Cathode Supply Voltage (V)
300 to 650	400 K	420	Bialkali	Borosilicate glass	Box-and-grid/10	1500	0.1	1250

Table 2
Specifications of plastic scintillator (Epic crystal).

Base Material	Density (g/cm^3)	Cleavage Plane	Soften Temperature (K)	Wavelength of Emission Max (nm)	Primary Decay Time (ns)	Light Output (%relatively of Anthracene)	H/C Ratio	Refractive Index
Polystyrene	1.05	no	348	415	2.40	50~60	1.10	1.58

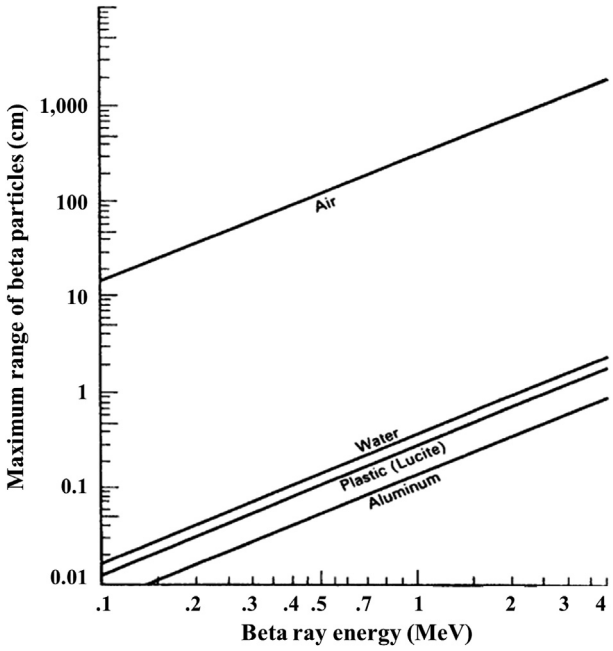

Fig. 3. Range-energy curves for beta particles in various substances.

2.2. Monte Carlo N-particle code simulation of the scintillator

The efficiency of the plastic scintillator was calculated using MCNP 6 [15]. Two types of plastic scintillators with thicknesses of 1 mm and 5 mm were evaluated. The 1-mm-thick scintillator was impossible to use because its mechanical strength was weak. The modeled system in which the plastic scintillator is placed on the vial that contains the source is shown in Fig. 6, and its material composition is given in Table 3 [16].

Beta-emitting radionuclides such as ^{3}H, ^{14}C, ^{32}P, and ^{90}Sr/^{90}Y were employed in the simulation. ^{90}Sr/^{90}Y was modeled to be in the equilibrium state with a ratio of 1:1. The maximum energies of ^{3}H^{14}C, ^{32}P, and ^{90}Sr are, 1.86E-02, 1.57E-01, 1.71E+00, and 2.28E+00 MeV [17], respectively. The range in air is 6, 24, 609, and 1062 mm for ^{3}H, ^{14}C, ^{32}P and ^{90}Sr, respectively; the corresponding ranges in water are 6, 0.28, 0.85, and 1.1 cm.

MCNP6 is designed to track several types of particles over a wide energy range. Because the MCNP did not consider the scintillation process, the efficiency of the plate was determined by the energy deposition of the beta particles using the F8 tally. Non-zero energy deposition of beta particles in the scintillator is considered as counts.

2.3. Sensitivity quantification and analysis of accuracy and uncertainty by manufacturing liquid open radioactive source

To quantify the sensitivity and analyze the accuracy and uncertainty of the system, open beta radioactive sources such as ^{3}H, ^{14}C, ^{32}P, and ^{90}Sr were prepared. For convenience of use, these sources were transferred to the vial and the mass of the transferred radioactive material was confirmed by using an electronic precision scale.

The procedure for manufacturing the beta radionuclide sources is as follows.

1. Extract 500 μL of each radioactive source and transfer to individual vials.
2. Check the mass of the extracted source using an electronic precision scale.
3. Dilute the extracted source with 5500 μL of water.
4. Measure the mass of the sample containing water and radioactive source using an electronic precision scale.
5. Seal the vial using nylon wrapping film.

Table 4 presents the information pertaining to the manufactured

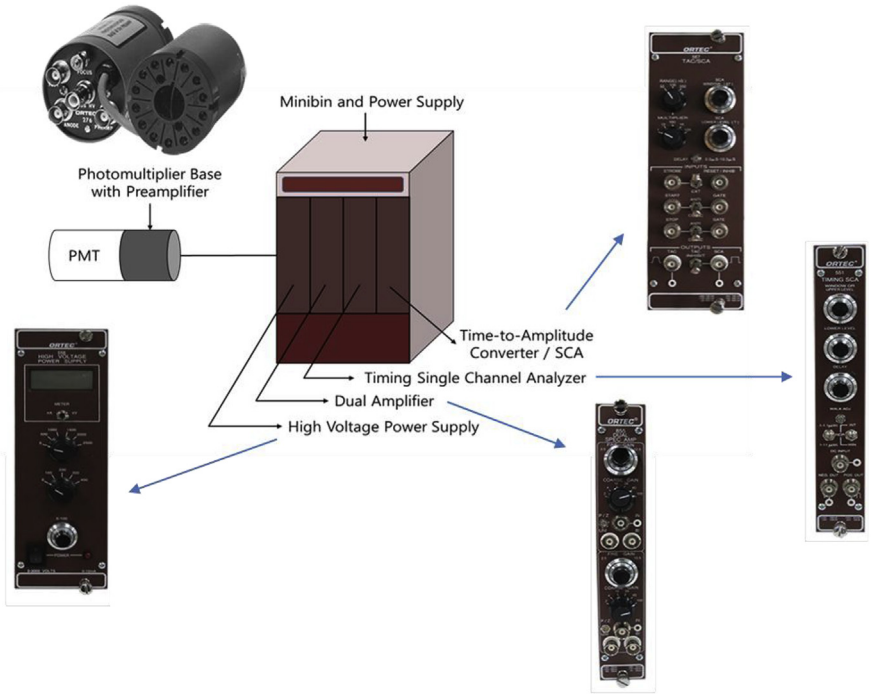

Fig. 4. Configuration of electronic system.

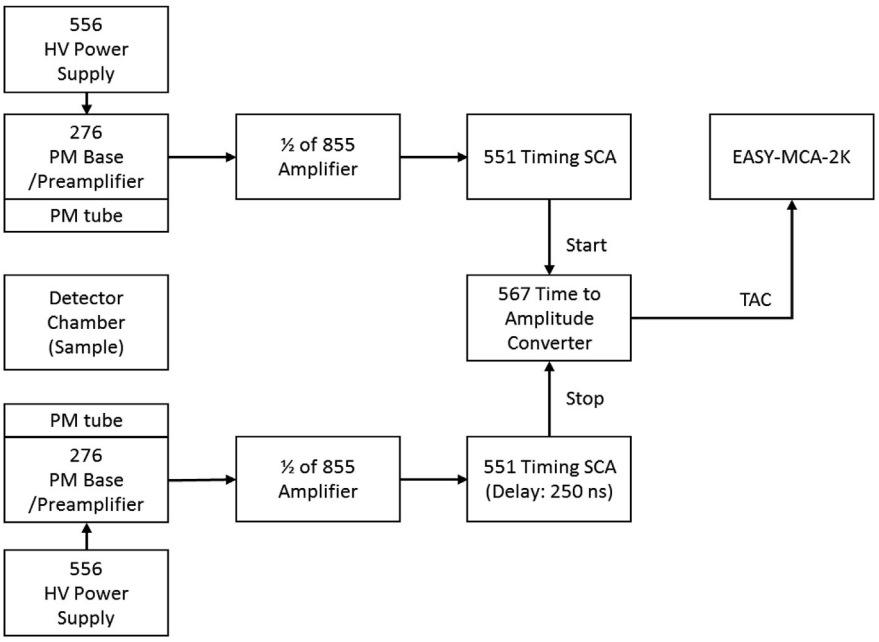

Fig. 5. Configuration of detection signal processing system.

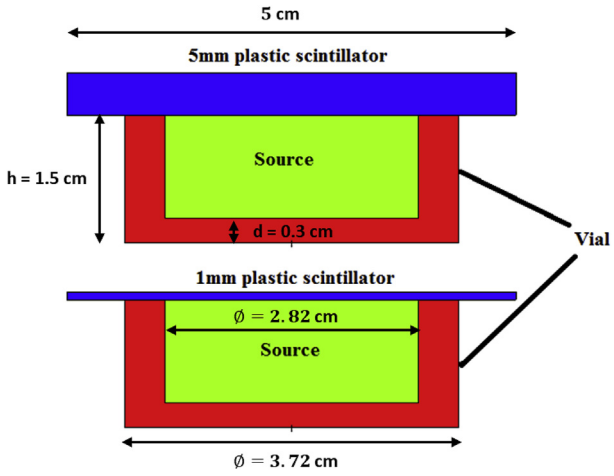

Fig. 6. Modeling of plastic scintillator with two different thicknesses: 1 mm and 5 mm.

single beta radionuclide sources (^{3}H, ^{14}C, ^{32}P, and ^{90}Sr) such as their initial radioactivity, mass, and date of manufacture [18]. The measurement time was 600 s.

The measurement uncertainty was derived from equation (3) [19].

$$u = \frac{s}{\sqrt{n}} \tag{3}$$

where u is the measurement uncertainty, s is the standard deviation, n is the number of measurements.

Table 3
Material component used for simulation.

Component	Composition	Density (g/cm^3)
Plastic scintillator	Polystyrene	31.05
Vial	Polyethylene	0.93
Source	Approximate by water	1

3. Result and discussion

3.1. MCNP simulation results of the scintillator

The efficiency was not affected by the thickness of the plastic scintillator. The efficiencies of the 1-mm and 5-mm plastic scintillators were equal. This can be explained using Fig. 7. In both cases, the amount of deposition energy is different; however, any non-zero energy deposition of the beta particles in the scintillator is considered as one count in the MCNP F8 tally calculation. The simulation efficiencies for each radionuclide are described in Table 5.

The efficiency of ^{3}H was relatively low owing to the short range of the beta in water. The high efficiency of ^{90}Sr/^{90}Y was mainly owing to the high-energy beta particles emitted from ^{90}Y (E_{max} = 2.23 MeV). These results confirmed that the thickness of the plastic scintillator did not influence detection efficiency.

3.2. Single beta radionuclide detected spectra by plastic scintillator

The detected spectra before and after the background subtraction are shown in Fig. 8. As shown in Table 5, no value is available for ^{3}H because its gross count is 3,429, which is lower than the value of the blank sample (3,485). The gross count of ^{14}C is slightly larger than that of the background. The ^{32}P and ^{90}Sr/^{90}Y sources have a difference greater than 15 counts per second compared with the blank sample. Further, a good agreement is observed between the simulation and the experiment results, with the relative errors of 1.95% and 0.43% for ^{32}P and ^{90}Sr/^{90}Y (Table 5).

In addition, the measured spectrum was normalized and compared with the known spectrum of the radionuclides [20]. As seen in Fig. 9, the measured spectra shifted to the left compared with the known spectra owing to the self-attenuation of the beta particles in the aqueous environment before they interacted with the scintillator. The maximum energy point of ^{32}P shifted from 1.67 MeV to 1.44 MeV; this represented a relative change of 13.7%,

Table 4
Parameters of single beta ray emitting nuclide source.

	^{3}H	^{14}C	^{32}P	^{90}Sr
Initial radioactivity (Bq)	3.52E+08	3.90E+03	3.89E+03	3.90E+03
Mass of total source(g)	4.97E+00	5.01E+00	5.00E+00	5.00E+00
Date of production	2017.07.01	2017.07.01	2017.07.01	2017.07.01
Radioactivity concentration (Bq/g)	**7.08E+07**	**7.79E+02**	**7.77E+02**	**7.81E+02**
Mass of source case before sampling (g)	3.39E+01	9.44E+00	8.68E+00	7.38E+00
Mass of source case after sampling (g)	3.34E+01	8.92E+00	8.18E+00	6.88E+00
Extracted sample mass (g)	4.92E-01	5.17E-01	5.01E-01	5.01E-01
Radioactivity extraction (Bq)	**3.48E+07**	**4.03E+02**	**3.89E+02**	**3.91E+02**
Sample case mass (g)	4.94E+00	4.94E+00	4.91E+00	4.94E+00
Sample case + Water + Sample mass(g)	1.08E+01	1.10E+01	1.11E+01	1.09E+01
Water + Sample mass (g)	5.85E+00	6.03E+00	6.16E+00	5.99E+00
Radioactivity concentration (Bq/g)	**5.95E+06**	**6.69E+01**	**6.32E+01**	**6.53E+01**

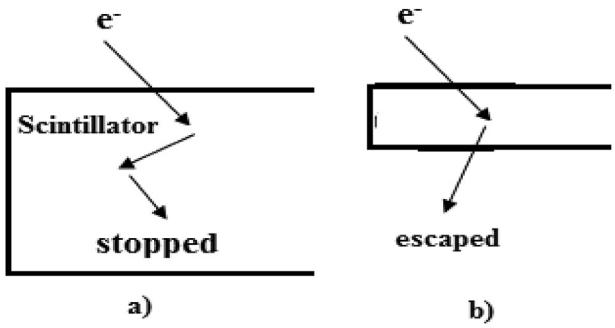

Fig. 7. Energy deposition of beta particles.

whereas the corresponding relative change for ^{90}Sr and ^{90}Y was 11.2%.

Although ^{3}H and ^{14}C spectra were not detected, it was predicted that these spectra would also be shifted to the left even more markedly than ^{32}P and $^{90}Sr/^{90}Y$. An important consequence of this shifted energy spectrum was that the photon distribution within the scintillator also changed. The reaction between the beta ray with the scintillator is hard because of beta ray's short range. It is also difficult to detect the generated photon because of the self-absorption in the scintillation. Therefore, further study is required to correct for the effects of the shifted light distribution considering the optical factors.

For ^{32}P and $^{90}Sr/^{90}Y$, which are high-energy beta nuclei, the difference was greater than 15 counts and 37 counts per second compared with the blank sample, and the relative measurement uncertainty values were 0.78% and 1.17%, respectively.

3.3. *Effect of water depth and scintillator diameter on detection efficiency*

The detection efficiency was calculated according to the diameter of the scintillator and the height of the water sample by nuclide through MCNP 6. As shown in Fig. 10, as the height of the water sample increased, the detection efficiency decreases and the

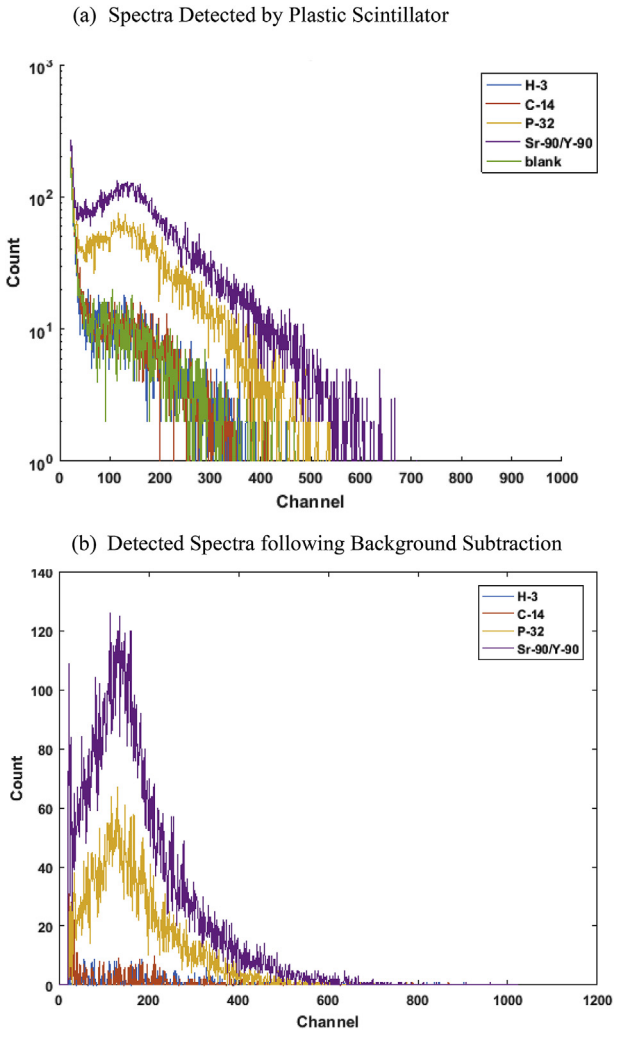

Fig. 8. Detected spectra for a single radionuclide.

Table 5
Detection results and relative difference between detection and simulation efficiency.

Radionuclides	Gross count (#)	Net counts (#)	Detection Efficiency (%)	Simulation efficiency (%)	Relative difference (%)
Background	3.49E+03	–	–		–
^{3}H	3.43E+03	Not available	Not available	2.00E-03 ± 4.70E-02	Not available
^{14}C	3.73E+03	2.41E+02 ± 8.50E+01	1.00E-01 ± 4.00E-02	1.07E-01 ± 7.00E-03	6.54E+00
^{32}P	1.27E+04	9.22E+03 ± 1.12E+02	5.54E+00 ± 7.00E-02	5.65E+00 ± 1.00E-03	1.95E+00
$^{90}Sr/^{90}Y$	2.51E+04	2.16E+04 ± 1.58E+02	4.60E+00 ± 3.00E-02	4.62E+00 ± 2.00E-03	4.30E-01

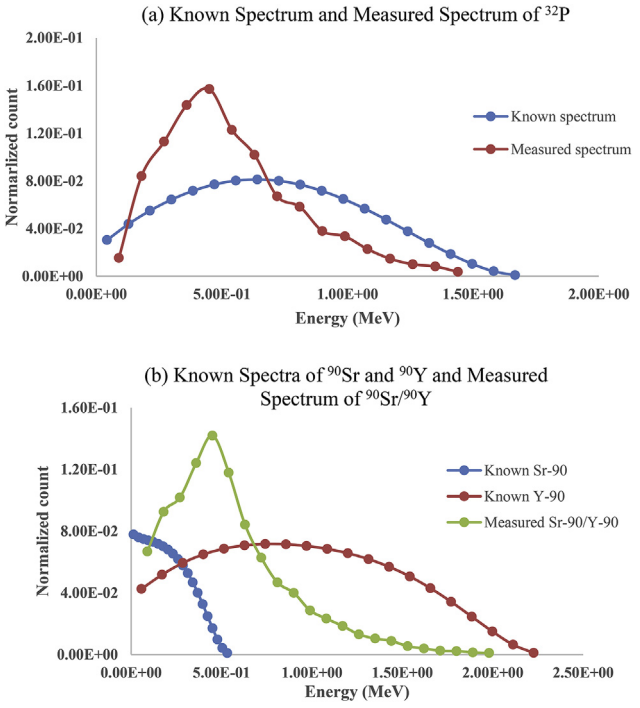

Fig. 9. Comparison between measured and known spectra of ^{32}P, ^{90}Sr, and ^{90}Y.

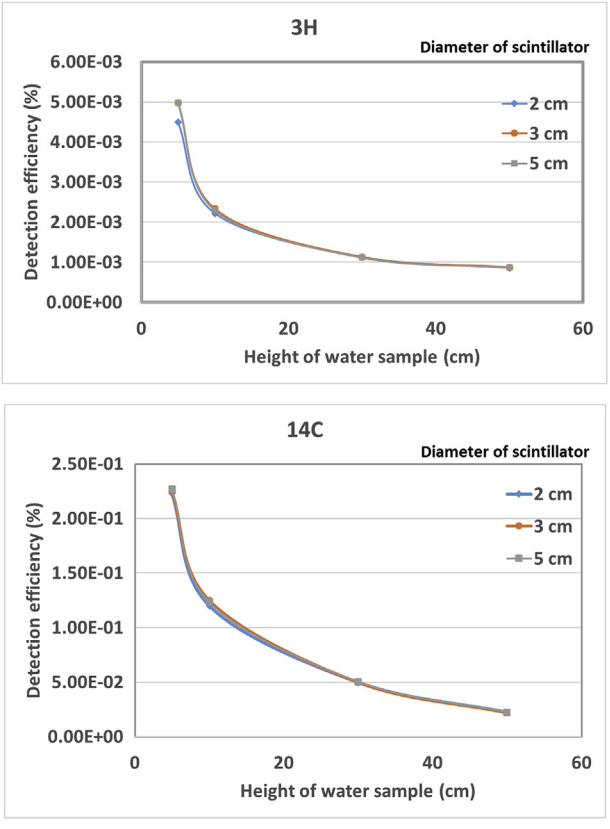

Fig. 10. Detection efficiency according to scintillator diameter and height of water sample.

influence of the diameter of the scintillator can be neglected. For the same scintillator diameter, as the water depth increases, the amount of the sample also increases. This leads to a decrease in radioactivity concentration. Further, because of the self-absorption effect of water, only the beta radionuclide directly in contact with the scintillator is measured. Therefore, it is considered that the detection efficiency decreased as the water depth increased.

4. Conclusion

An in situ groundwater beta nuclide detection system using plastic scintillation was developed in this study. No additional cost was required to monitor beta nuclides in water, because the measurement was performed by allowing the water sample to directly flow into the detector. Furthermore, no pretreatment is necessary for measurement, and secondary wastes are not generated. Moreover, because the problem of contamination spread does not occur between the samples during sampling, water samples can be efficiently monitored in nuclear facilities.

The efficiency of the plastic scintillator was calculated based on MCNP 6 simulation and experimental tests. A 1-mm thick plastic scintillator could be used in an in situ system. The simulation and experimental results showed good agreement. The low counting efficiency for ^{3}H and ^{14}C was due to the short range of their low-energy beta particles in water. Furthermore, the spectral shift was more significant for low-energy beta particles and would hinder qualitative identification as well as quantification of these radionuclides. For ^{32}P and ^{90}Sr/^{90}Y, which are high-energy beta nuclei, the relative measurement uncertainty values were 0.78% and 1.17%, respectively, which are not critical values. A 5-cm diameter offered a shorter measuring time compared with the smaller diameters. The water depth can affect the detection efficiency owing to the self-absorption effect.

In summary, the fundamental and experimental approaches for applying a plastic scintillator to an in situ beta monitoring system were conducted. It was confirmed that plastic scintillator can react with major beta-emitting nuclides. Therefore, it can be used for monitoring at a decommissioning site. Further research on the efficiency of the detection system is needed, with a focus on radionuclides that emit weak beta particles.

Acknowledgments

This work was supported by the National Research Foundation of Korea grant funded by the Korean government (MSIP: Ministry of Science, ICT and Future Planning) NRF-2016M2B2B1945082.

Appendix A. Supplementary data

Supplementary data to this article can be found online at https://doi.org/10.1016/j.net.2019.05.006.

References

[1] S.W. DUCE, et al., In situ radiation detection demonstration, in: WM'00 Conference, Tucson, AZ, February 27, March 2 2000.
[2] S.J. Ko, et al., Radiation Detection & Measurement, 2001 (in Korean language).
[3] J.W. Coltman, F.H. Marshall, Photomultiplier radiation detector, Nucleonics 1 (3) (1947) 58–64.
[4] B.K. Seo, Z.H. Woo, G.H. Kim, K.W. Lee, D.G. Lee, Development of ZnS (Ag)/plastic dual scintillator sheet for simultaneous alpha-and beta-ray counting, Anal. Sci. Technol. 21 (2) (2008) 117–122.
[5] HAMAMATSU, Photomultiplier Tube R878". www.hamamatsu.com.
[6] Saint-Gobain Crystals, Organic Scintillation Materials, 2014.
[7] L.A. Eriksson, C.M. Tsai, Z.H. Cho, C.R. Hurlbut, Comparative studies on plastic scintillators—applications to low energy high rate photon detection, Nucl. Instrum. Methods 122 (1974) 373–376.
[8] American Society for Testing and Materials, Standard Practice for the Measurement of Radioactivity.
[9] H. Cember, T.E. Johnson, "INTRODUCTION TO Health Physics", Medical, 2009.
[10] Ortec Inc. "Model 556H High Voltage Power Supply Operating and Service

Manual".
[11] Ortec Inc. "Model 855 Dual Spectroscopy Amplifier Operating and Service Manual".
[12] Ortec Inc. "Model 551 Timing Single-Channel Analyzer Operating and Service Manual".
[13] Ortec Inc. "EASY-MCA-8KTM EASY-MCA-2ktm Digital Gamma-Ray Spectrometer User's Manual".
[14] Ortec Inc, Experiment 13, Gamma-Gamma Coincidence with Angular Correlation. www.ortec-online.com.
[15] T. Goorley, M. James, T. Booth, F. Brown, J. Bull, L.J. Cox, J. Durkee, J. Elson, M. Fensin, R.A. Forster, J. Hendricks, Initial MCNP6 release overview, Nucl. Technol. 180 (3) (2012) 298–315.
[16] R.G. Williams, C.J. Gesh, R.T. Pagh, Compendium of Material Composition Data for Radiation Transport Modeling, Pacific Northwest National Lab.(PNNL), Richland, WA (United States), 2006 Oct 31.
[17] Ministry of Education, Science and Technology, "Radionuclide information", 2008 (in Korean language).
[18] ALAEI, Parham, Introduction to health physics, Med. Phys. 35 (12) (2018), 5959-5959.
[19] Korea Research Institute of Standards and Science, Instruction for Expressing Measurement Uncertainty, 2010 (in Korean language).
[20] W.G. Cross, C.G. Soares, S. Vynckier, K. Weaver, Dosimetry of beta rays and low-energy photons for brachytherapy with sealed sources, ICRU report 72, J. ICRU 4 (2004). J ICRU.